



Biogenic synthesis of silver nanoparticles using S1 genotype of *Morus alba* leaf extract: characterization, antimicrobial and antioxidant potential assessment

Dipayan Das¹ · Raja Ghosh² · Palash Mandal¹

© Springer Nature Switzerland AG 2019

Abstract

Present study deals with synthesis and assessment of antimicrobial and antioxidant activity of silver nanoparticles using aqueous extract of mulberry leaves. The optical study showed the appearance of SPR peak in the range of 423–450 nm affirming nanosilver formation. FTIR analysis indicates the possible involvement of proteins, carbohydrate and secondary metabolites as reducing and capping agents. SEM, TEM and HR-TEM analysis reveals that the synthesized nanoparticles were spherical in shape with particle size ranges between 12 and 39 nm. EDX spectra showed maximum intensity at 3 keV, affirming silver crystal. XRD analysis showed silver nanoparticles were preferentially oriented along (111) revealing crystalline structure. DLS analysis confirms the stability of silver nanoparticles with zeta potential of + 37.4 mV. Silver nanoparticles showed effective antimicrobial activity against both gram positive and gram negative bacteria with highest activity against *Salmonella typhimurium* with MIC 40 µg/ml. Further silver nanoparticles also showed dose dependent antioxidant activity against free radicals like DPPH, ABTS⁺, superoxide and nitric oxide; besides this nanosilver also performed significant metal chelating activity.

Keywords Silver nanoparticles · Mulberry leaf extract · Characterization · Antimicrobial · Antioxidant

1 Introduction

Biogenic method of synthesis of metal nanoparticles are increasingly becoming popular in present day world due to their simplicity, less toxic, effortless and eco-friendly nature. Copper, zinc and silver are mostly used metals for synthesis of nanoparticles because of their biomedical properties [1]. Silver nanoparticles is increasingly becoming popular and faces an annual demand of five hundred tons [2] due to its non-toxic, optical, catalytic, bio-sensing, drug delivery, antioxidant, cytotoxic and antimicrobial activities [3, 4]. Literature study reports several techniques including chemical reduction [5], thermal decomposition [6, 7], photochemical reduction [8], heat evaporation [9] and microwave irradiation [10] for the formation of silver

nanoparticles. Most of these techniques are costly, toxic and requires chemical compounds which put harmful effect on living system, imposing an extra demand for finding alternative technique that utilizes nontoxic natural compounds for nanosilver production.

Biogenic method uses microorganism both living and dead [11, 12], fungi [13], leaf extract [14], root extract [15], fruit extract [16, 17], latex [18], enzymes [19–21] and many others for the preparation of bio-friendly silver nanoparticles. Plant extract gain extra advantage over microorganism, as isolation and maintenance of microbial culture under aseptic condition was not cost effective [22]. Besides the rate of production of nanoparticles using microorganisms was much slower than plant mediated synthesis [23]. Plant extracts that were reported recently in biosynthesis

✉ Palash Mandal, pmandalbotppprl@nbu.ac.in | ¹Plant Physiology and Pharmacognosy Research Laboratory, Department of Botany, University of North Bengal, Raja Rammohunpur, Siliguri, West Bengal 734013, India. ²Department of Chemistry, University of North Bengal, Raja Rammohunpur, Siliguri, West Bengal 734013, India.



of silver nanoparticles included *Datura stramonium* [24], *Moringa stenopetala* [25], *Cymbopogon citratus* [26], *Casia roxburghii* [27], *Bergenia ciliata* [28], *Cardiospermum halicacabum* [29], *Carica papaya* [30], *Eclipta alba* [31] and many others.

We have selected leaf extract of *Morus alba* (Mulberry), plant which bears not only economic importance but also having medicinal importance. Wild and cultivated species of mulberry are distributed throughout India [32], making their easy availability. Global importance of mulberry is the utilization of its leaves for the feeding of monophagous insect *Bombyx mori*. Mulberry is also used for its anti-diabetic [33], antimicrobial [34], antioxidant [35, 36], neuro-protective [37], anticancerous [38] and hepatoprotective [39] activity. Because of its high medicinal importance, mulberry leaves along with its root and stem are consumed directly as tea in different parts of world [40, 41].

Earlier workers have biosynthesizing silver nanoparticles using dried mulberry leaf extract, which was either sun dried [42] or shade dried [43, 44]. Oxidative change in phytochemical constituents may occur during drying process, which may put significant impact in reduction process during nano formation. To avoid such possibility, we aimed in using aqueous decoction of fresh mulberry leaves through refluxing for nanosilver formation.

Current work is based on the hypothesis that synthesized nanoparticles will bear effective antimicrobial and antioxidant activity. Present approach deals with biosynthesis of silver nanoparticles using mulberry leaf extract that will act as reducing and stabilizing agent. The synthesized nanoparticles will be characterized for determining nature, type, morphology, shape and functional groups involved in nanoparticles formation. The antimicrobial activity of synthesized nanoparticles will be screened by studying the zone of inhibition and MIC of both gram positive and gram negative bacteria and antioxidant scavenging potential will be screened through DPPH, ABTS⁺, nitric oxide, superoxide and metal chelating activity.

2 Materials and methods

2.1 Preparation of plant extract

Fresh, mature and disease free S1 genotype of mulberry leaves were collected from Matigara Sericulture Complex, Siliguri, West Bengal, India (26°70'40"N and 88°35'37"E). The leaves were surface cleaned with double distilled water several time to remove the debris and organic contaminants and were then air dried for 45 min to remove the water content at room temperature. About 10 g leaves were finely chopped and refluxed with 100 ml double distilled water for 60 min. The yellowish aqueous extract was

filtered out with Whatman No. 1 filter paper (GE Healthcare UK Ltd, China make) and then centrifuged at 2000 rpm for 5 min to remove suspended impurities. The supernatant was used for biogenic synthesis of silver nanoparticles.

2.2 Synthesis of silver nanoparticles

For synthesizing silver nanoparticles, 10 ml plant extract was added drop wise to 90 ml aqueous solution of silver nitrate (SIGMA-ALDRICH Batch # 0000003756) with continuous uniform stirring for 10 min using magnetic stirrer (REMI EQUIPMENTS). The reducing and capping agents present in the extract changes the colour of the solution from transparent to reddish or blackish brown, indicating the formation of silver nanoparticles.

2.3 Characterization of silver nanoparticles

2.3.1 UV-visible spectra analysis

Initial characterization of reduction of Ag⁺ ion was done after 12 h of reaction by diluting the nano solution in 1:4 ratio and by plotting absorption spectra against wavelength range of 300–800 nm using UV-Vis Spectrophotometer (SYSTRONICS-2201).

2.3.2 Fourier transformed infrared spectroscopy (FTIR)

Detection of functional groups for predicting the involvement of organic molecules as reducing and capping agents for reduction of silver ion was done using Fourier Transformed Infrared Spectroscopy (THERMO NICOLET, AVATAR 370), with a wavelength range of 4000–500 cm⁻¹ and a resolution of 4 nm. Dried nanoparticles and plant extract were incorporated directly on potassium bromide crystals to obtain the spectra in transmittance mode.

2.3.3 Scanning electron microscopy (SEM) and field emission scanning electron microscope (FESEM)

SEM and FESEM analysis was conducted for studying the shape and surface morphology of synthesized nanoparticles. SEM analysis was done using JEOL Model JSM-6390LV SEM machine. For analysis, drop of sample was dried on a carbon-coated copper grid and then images were taken at different magnification. FESEM was analyzed with JEOL Model JSM-7600F at an accelerating voltage of 10 kV and at 50,000× magnification.

2.3.4 Energy dispersive X-ray spectroscopy (EDX)

EDX analysis was performed for determining the elements present in the synthesized nanoparticles. EDX analysis was

done on dry sample through Oxford-EDX system that uses 80 mm² SDD detector that detects element under high resolution.

2.3.5 High resolution transmission electron microscopy (HR-TEM)

HR-TEM was analyzed was done using FEI TECNAI G2, F30 by operating at an accelerating voltage of 300 kV. HR-TEM analysis was done for determining the size, shape and morphology of silver nanoparticles. The size distribution range was obtained using Origin b9.5.5.409 software (Origin Lab Corporation, USA) by measuring the size of more than 350 particles. Percent polydispersity of synthesized nanoparticles was determined using the following formula: Polydispersity (%) = $(\sigma/x_c) \times 100$, where σ = standard deviation of particle size distribution and x_c = average nanoparticles size.

2.3.6 X-ray diffraction analysis (XRD)

For determining X-ray diffraction pattern, centrifuged and dry crystals of silver nanoparticles were used. XRD analysis was done using BRUKER AXS D8 ADVANCE (BRUKER KAPPA APEX II) machine, operated at 30 mA current and at 40 kV voltage. For generating 2θ data the sample was Cu K α radiated, operated at a speed of 5°/min. The result obtained was compared with standard JCPDS library for determining the crystalline structure. The average crystalline size has been estimated using Debye–Scherrer's formula, $D = (0.9\lambda/\beta\cos\theta)$ where λ is the wavelength of the X-ray source, β is the angular FWHM of the XRD diffraction peak and θ is the Bragg angle. FWHM was calculated from Gaussian function using Origin b9.5.5.409 software. Inter planar spacing (d) was calculated from Bragg's Law, $2d\sin\theta = n\lambda$ where n is the order of diffraction pattern. Lattice constant (a_0) has been derived from the following formula, $a_0 = d \times \sqrt{(h^2 + K^2 + l^2)}$, where d is inter planar spacing and h, k, l are plane direction.

2.3.7 Dynamic light scattering (DLS)

DLS analysis of synthesized nanoparticles was done to correlate relationship between particle size and number of particles. Through DLS study zeta potential and average particle size of synthesized nanoparticles was determined. Measurement was done through DLS analyzer (ZETASIZER NANO ZS90 ZEN3690) where water was used as dispersion medium with dispersion and material refractive index of 1.332 and 1.330 respectively, viscosity of 0.8872 cP, count rate of 343.7 Kcps and temperature of 25 °C.

2.3.8 Antimicrobial activity

Disk diffusion method was followed for screening the antimicrobial activity of synthesized nanoparticles using mulberry leaf extract. Antimicrobial activity was tested at seven different concentrations of silver nanoparticles (25, 50, 100, 200, 300, 400, 500 µg/ml). Gram positive (*Bacillus megaterium* ATCC 14581, *Staphylococcus aureus* ATCC 11632, *Bacillus subtilis* ATCC 11774) and gram negative (*Escherichia coli* ATCC 11229 and *Salmonella typhimurium* ATCC 25241) test organisms were grown for 6 h on nutrient broth prior to their application to obtain rapidly growing viable cells. 100 µl test organism from nutrient broth was mixed uniformly with nutrient agar plate and was allowed to solidify. After 30 min, paper disk soaked with appropriate concentration of nanosilver was placed in the nutrient agar plate. The zone of inhibition was calculated in millimetre scale after 24 h of incubation at 37 °C.

Antimicrobial activity of silver nanoparticles was also evaluated in terms of minimum inhibitory concentration (MIC). For estimation, different concentration of silver nanoparticles was added to 50 ml sterilized nutrient broth and to it 0.1 ml actively growing viable bacterial culture was added maintained at 10⁶ CFU/ml. Microbial growth was measured using UV–visible spectrophotometer (SYSTRONICS-2201) at 600 nm after 24 h incubation at 37 °C and 120 rpm.

2.3.9 Antioxidant activity

Antioxidant activity of prepared nanosilver and plant extract was evaluated following standard protocol in terms of ABTS⁺ [45], DPPH [46], superoxide [47], nitric oxide [48] scavenging and metal chelating [49] activity. Scavenging and chelating activity was measured as percent inhibition using the following equation: Percent inhibition = $[(A_0 - A_1)/A_0] \times 100\%$, Where A_0 is the absorbance of the control and A_1 is the absorbance of the sample. Antioxidant activity was expressed as concentration where 50% reduction in free radical takes place referred to as IC₅₀ value.

3 Result and discussion

3.1 UV–visible spectra analysis

Biogenic synthesis of silver nanoparticles was confirmed by colour change of silver nitrate solution from transparent to yellowish and finally to reddish or blackish brown (Fig. 1). The dielectric medium and the organic constituents of the plant extract are few of many factors responsible for change in colour during nano formation

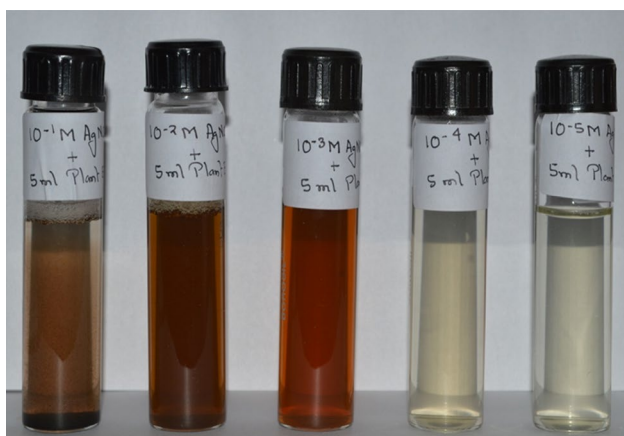


Fig. 1 Biogenic synthesis of silver nanoparticles mediated by mulberry leaf extract at different concentration of silver nitrate

[50]. Further validation of nanoparticles formation was done using UV-Vis spectrophotometer. Sastry et al. [51] reported that appearance of surface plasmon resonance (SPR) spectra in the wavelength range of 400–500 nm confirms the formation of silver nano particles. Figure 2 shows SPR spectra of silver nanoparticles formed using different concentration (2.5, 5, 10, 15, 20 ml) of plant extract keeping the concentration of silver nitrate constant (10^{-3} M). The characteristic UV-visible spectra shows SPR band of formed nanosilver at ~ 429 nm when synthesized using 2.5 ml plant extract. The obtained peak gets shifted towards red region when nano was prepared with 5 ml (~ 432 nm) and 10 ml (~ 432 nm) plant extract. However decrease in SPR spectra (blue shift) was noticed with increase in concentration of extract to 15 ml (~ 426 nm) and 20 ml (~ 423 nm). The red or blue shift of SPR spectra mainly depends on size, shape and nature of organic constituents present in surrounding medium [52]. The

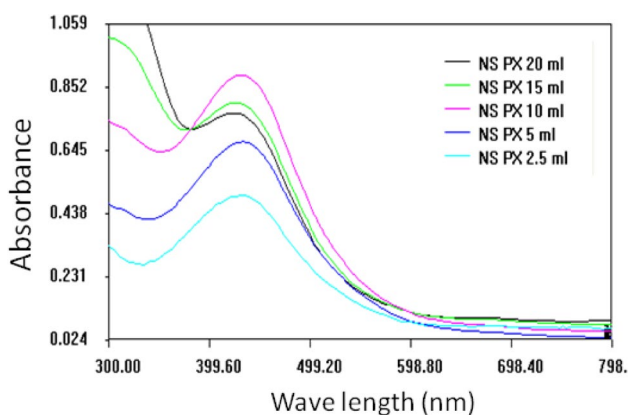


Fig. 2 UV-visible spectra of silver nanoparticles synthesized at different concentration of leaf extract

decrease in SPR spectra at high concentration of plant extract takes place because excess biomolecules beyond a certain limit ceases nano formation [53].

Nano synthesis was also monitored at different concentration of silver nitrate (10^{-1} , 10^{-2} , 10^{-3} , 10^{-4} , 10^{-5} M) keeping the concentration of plant extract constant in the ratio of 1: 9. The UV-visible spectrum (Fig. 3) shows SPR bands that range from 430 to 450 nm which confirms nano formation. It was observed that 10^{-4} M and 10^{-5} M concentration of silver nitrate was insufficient for nano formation, while at high concentration (10^{-1} M), formed nanoparticles in solution became hazy due to the reaction between excess concentration of silver nitrate with biomolecules, resulting in low intensity and broad SPR spectra. The broad and low intensity SPR band at high concentration appeared because of sedimentation of particle with time. Similar result was also reported by Balavijayalakshmi and Ramalakshmi [54] using *Carica papaya* peel. Nanosilver formed with 10^{-2} M and 10^{-3} M silver nitrate showed maximum wavelength peak at ~ 450 nm and ~ 435 nm respectively, indicating red shift with increase in concentration. SPR peak at high wavelength indicates large particle size [14]. Kaya et al. [55] reported that small size nanoparticles are biologically more active than large size nanoparticles. As nanosilver produced from 10^{-3} M silver nitrate shows SPR peak at lower wavelength than 10^{-2} M, so its particle size will be smaller than that produced by 10^{-2} M silver nitrate and thus is biologically more active.

3.2 Fourier transformed infrared (FTIR) spectroscopy

FTIR analysis was conducted to determine possible involvement of functional groups participating in reduction and stabilization of silver nanoparticles. FTIR spectra of dried aqueous plant extract showed absorption band

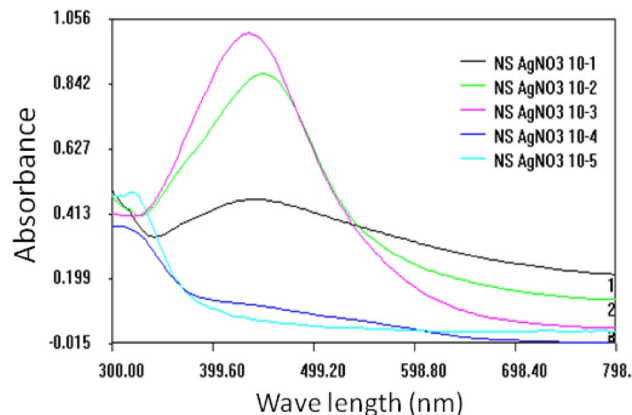


Fig. 3 UV-visible spectra of silver nanoparticles synthesized at different concentration of silver nitrate

at 3425.1, 1627.7, 1386.6, 1066.4, 1020.2, 761.7, 572.7 and 518.7 cm^{-1} (Fig. 4a). After reduction, certain spectral peaks showed slight shift in wave number such as 3430.9, 1033.7 and 796.4 cm^{-1} ; bands at 1627.7, 1386.6, 572.7 and 518.7 cm^{-1} appeared at exact location, while two extra band appeared at 2919.8 and 2854.2 cm^{-1} (Fig. 4b). The spectral similarity between plant extract and nano silver with minor deviation due to reduction process [56] strongly supports the involvement of different components of plant extract in bioreduction of metallic salts into nanoparticles. Ganesh Babu and Gunasekaran [57] reported that interaction between metal salts and biomolecules for the production of nanoparticles takes place through the involvement of functional groups. The bands at 3425.1 cm^{-1} shifted to 3430.9 cm^{-1} corresponds to N–H vibration mode which was overlapped with –OH vibration stretching of alcoholic and phenolic compounds [22, 58]. The peaks at 2919.8 cm^{-1} and 2854.2 cm^{-1} represents vibrations of –CH₂ and –CH₃ functional groups. These peaks are not detected in plant extract probably due to interference of –OH vibration stretching. Strong intense peak at 1627.7 cm^{-1} corresponds vibration of primary and secondary amines [59, 60] and 1386.6 cm^{-1} corresponds to C–N vibration stretch, probably representing amide I band of proteins found in leaf extracts [61]. The intense band at 1066.4, 1020.2 cm^{-1} of plant extract and 1033.7 cm^{-1} of nano silver represents strong C–O– and C–OH stretching vibration of carboxylic acid, alcohol, ester and ether bond of protein and carbohydrate present in the extract [62, 63]. Peak at 761.7 cm^{-1} of extract was shifted towards higher wave number at 796.4 cm^{-1} in prepared nanosilver indicates N–H vibration of primary aliphatic amines. Absorption band at 572.7 and 518.7 cm^{-1} indicates C–Cl stretching vibration and C–C skeleton vibration of branch

alkenes respectively. Butt et al. [64] reported the presence of protein, carbohydrate, glycoprotein, phenols, flavonoids, aminoacids, carotene and anthocyanins in mulberry leaf extract. Liang et al. [65] through spectroscopic analysis detected the presence of glucose and sucrose as carbohydrate; alanine, asparagines, GABA and proline as amino acid; acetic acid and succinic acid as a mono and di-carboxylic acid respectively; trigonelline as alkaloid in mulberry leaf extract. Hunyadi et al. [66] reported the presence of secondary metabolites like chlorogenic acid, rutin, isoquercitrin in mulberry leaf extract. Thus the functional groups detected in IR spectra, defines the presence of carbohydrate, proteins and different secondary metabolites in the plant extract that are involved in reduction of silver ion and also acts as stabilizing agent.

3.3 Scanning electron microscopy (SEM) and Field emission scanning electron microscope (FESEM)

SEM micrograph of biosynthesized silver nanoparticles was given in Fig. 5a. From SEM imaging it was observed that most of the silver nano particles were spherical while some are irregular in shape. The micrograph obtained in FESEM (Fig. 5b) also shows spherical nanoparticles, supporting the result obtained by SEM. Uniform alignment of silver nanoparticles was observed in FESEM with average particle size of 16.33 ± 5.14 nm. The particle size distribution ranges from 12 to 40 nm, some particles of size greater than 50 nm were also observed but are probably due to the overlapping of one particle with another. In some places particles were agglomerated due to cross linking [52] or may be due to evaporation of solvent during preparation of sample [67].

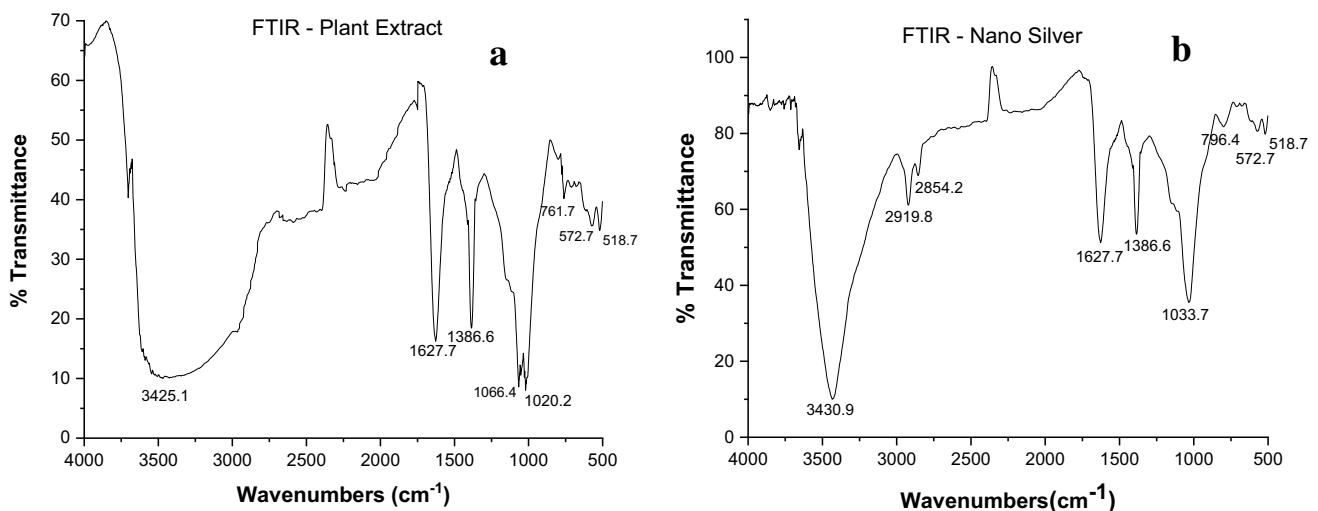


Fig. 4 FT-IR spectra of **a** mulberry leaf extract and **b** biosynthesized silver nanoparticles

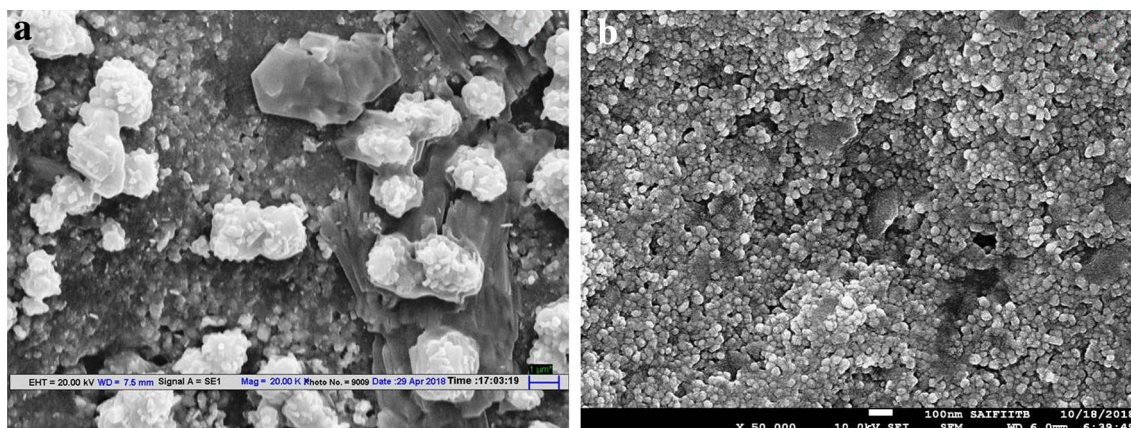


Fig. 5 **a** SEM and **b** FESEM micrograph of biosynthesized silver nanoparticles

3.4 Energy dispersive X-ray spectroscopy (EDX)

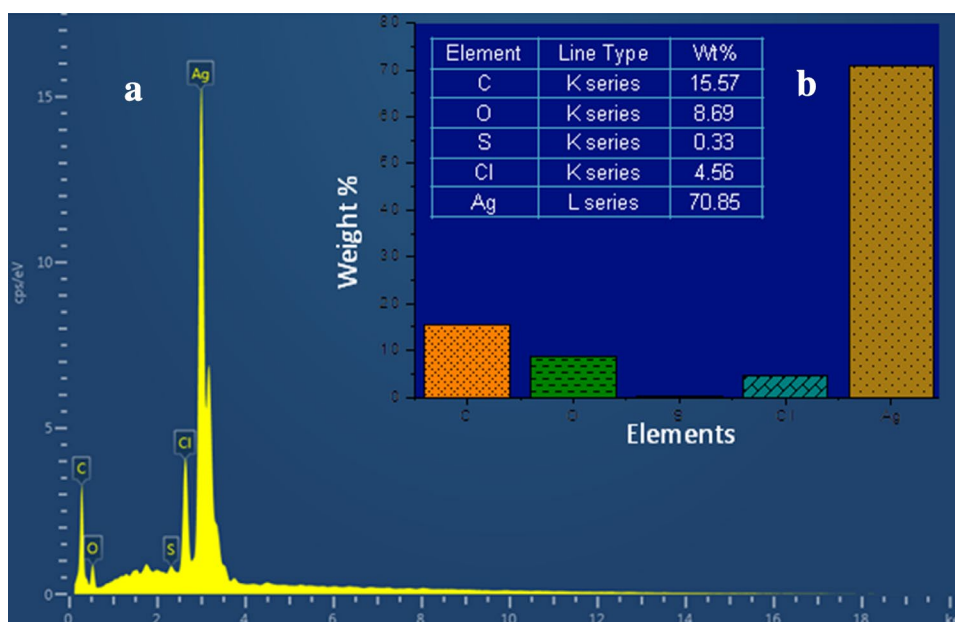
For identifying the elements involved in synthesis of silver nanoparticles, energy dispersive spectrum analysis was conducted. EDX analysis gives both qualitative and quantitative information regarding the participation of element in bioreduction. The elemental profile shows the presence of C, O, S, Cl and Ag (Fig. 6a), with strong intensity peak at 3 keV representing Ag. Due to surface plasmon resonance, silver shows intense peak at 3 keV confirming the formation of silver nanoparticles [68, 69]. The quantitative profile of elements in terms of percent weight indicated that silver accounting maximum portion ~70% followed by carbon and oxygen (Fig. 6b). Presence of carbon and oxygen indicates the presence of alkyl chain as stabilizing agent during the bioreduction

of metallic silver [70], supporting the result obtained through FTIR analysis.

3.5 High resolution transmission electron microscopy (HR-TEM)

From HR-TEM images it was observed that formed silver nanoparticles were spherical in shape and they vary in their size distribution. HR-TEM image of prepared nanosilver at 200 nm scale was represented in Fig. 7a. From HR-TEM study average particle size was estimated to be 14.95 ± 2.29 nm and size distribution ranges between 12 and 38 nm (Fig. 7b). The variation in size distribution was mainly due to clustering of nanoparticles at some places [67]. TEM analysis reveals that the periphery of the nanoparticles is thinner than centre, indicating the involvement

Fig. 6 **a** EDX spectra and **b** elemental profile of biosynthesized nanoparticles



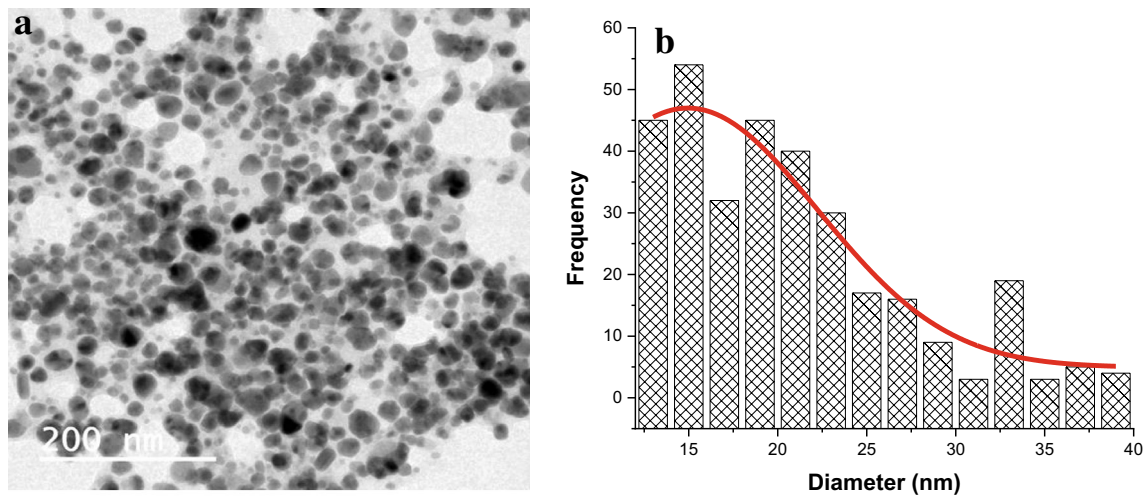


Fig. 7 **a** HR-TEM micrograph of biosynthesized silver nanoparticles and **b** particle size distribution

of protein molecules as capping agent [71]. The polydispersity was found to be 11.35% indicating that most of the particles remain in monodispersed phase; similar finding had been reported by Ibharim [72] and Banala et al. [30] using banana peel and papaya leaf extract respectively. Application of nanoparticles largely depends on size, shape and polydispersity index of particles [73]. Agnihotri et al. [74] reported that bioactivity of silver nanoparticles, mainly antimicrobial activity is inversely proportional to the size of the nanoparticles. Present study represents smaller size nanoparticles, supporting their bioactive nature.

3.6 X-ray diffraction analysis (XRD)

For confirming the crystalline nature of biologically synthesized nanoparticles, XRD pattern of dried nanosilver was studied and was represented in Fig. 8. Four prominent diffraction peak were obtained at 38.14° , 44.26° , 64.46° , 77.41° corresponding to (hkl) values of (111), (200), (220), (311) Bragg's reflections plane of face centered cubic silver. The obtained data was matched with standard JCPDS library file no: 04-0783 which also confirms face centered cubic structure of biosynthesized silver nanoparticles. The intensity of peak at (200), (220) and (311) are weak and are broad, while (111) represents sharp and intense peak indicating that nanocrystals are (111) oriented. By determining Debye–Scherrer's equation at (111) Bragg's reflection, the average crystalline size was found to be 10.65 nm. Similar XRD orientation was earlier reported by Awwad et al. [3] and Premasudha et al. [31] while synthesizing silver nanoparticles using Carob and *Eclipta* leaf extract respectively. Besides normal peaks of silver, three extra peaks at 27.86° , 32.26° and 46.11° were observed and these peaks

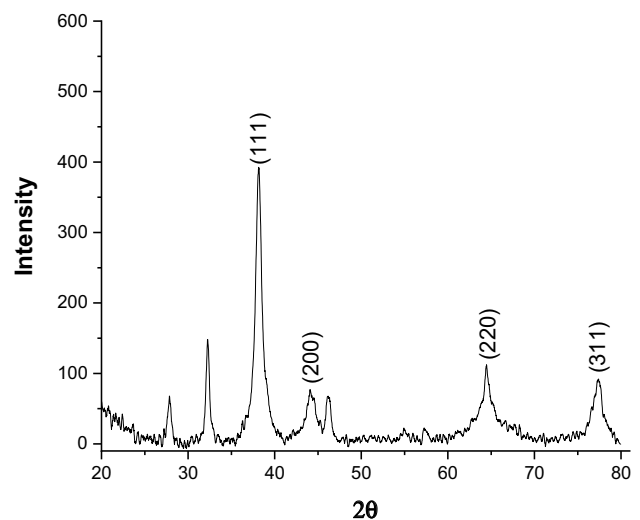


Fig. 8 XRD pattern of silver nanoparticles synthesized from mulberry leaf extract

represents the organic constituents of extracts that are responsible for reduction of silver ion [75].

The crystalline nature of synthesized nanoparticles was further evaluated through selected area electron diffraction (SAED) pattern (Fig. 9). The bright diffraction spots corresponds to (111), (200), (220) and (311) Bragg reflection planes [76]. SEAD pattern reflects that the crystals are mostly oriented on (111) plane and due to which sharp and intense peak was generated at (111) XRD pattern.

The FWHM value, crystalline size (D), dislocation density (δ), inter planar spacing (d), lattice constant (a_0) and cell volume against Bragg's reflections at (111), (200), (220) and (311) are represented at Table 1. The obtained lattice constant value of most intense peak (111) was 4.084 \AA which

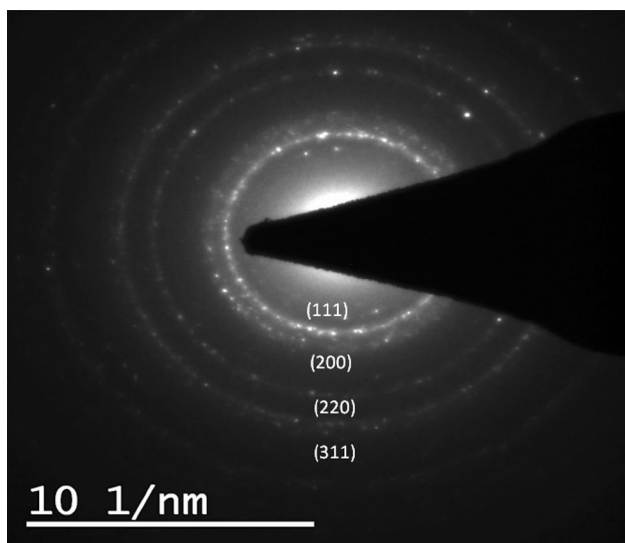


Fig. 9 SAED image of biosynthesized silver nanoparticles

almost matches exactly with the reported standard value of silver which is 4.086 Å (JCPDS file no: 04-0783). Similar finding on biogenic synthesis of silver nanoparticles was earlier reported by Anandalakshmi et al. [77] and Mehta et al. [78].

3.7 Dynamic light scattering

DLS analysis reveals that all the particles in the dispersion remain in nano-size with average zeta diameter of 29.68 nm and polydispersity index (PDI) of 0.441 (Fig. 10). The particle size obtained from DLS analysis is greater than that obtained through TEM and XRD analysis, this may be due to the fact that DLS analysis takes into consideration associated capping and reducing agents during size measurement [79]. Besides size for biological activity, stability of nanoparticles plays an important role [80]. Nano stability is measured in terms of zeta potential which measures the surface charge of nanoparticles. Nanoparticles bearing greater positive or negative zeta potential will repulse each other, which will prevent nano agglomeration and there by increases stability [81]. Particles bearing zeta potential greater than + 30 mV or less than – 30 mV are considered to remain stable without agglomeration for longer duration [82]. The zeta potential value of biosynthesized silver

nanoparticles was + 37.4 mV, indicating that the particles are present in highly stable state. Positive value of zeta potential was due to development of electrostatic force of attraction between positively charged capping agents with the nanoparticles [83].

3.8 Antimicrobial activity

Biosynthesized silver nanoparticles using mulberry leaf extract showed potent antimicrobial activity against both gram positive and gram negative bacteria as evident by measuring the diameter of inhibition zone (Fig. 11). The data tabulated in Table 2 indicates that at maximum concentration (500 µg/ml) silver nanoparticles showed highest activity against gram positive bacteria, *Bacillus megaterium* (22.03 ± 1.06 mm) while at lowest concentration (25 µg/ml) best activity was obtained against gram negative bacteria, *S. typhimurium* (10.51 ± 1.17 mm) than other tested microorganisms. This result was possibly due to the fact that metals at higher concentration can easily bind to the surface of gram positive bacteria [84], while at lower concentration thick peptidoglycan layer, consisting of linear polysaccharide chains cross linked by short peptides makes the cell wall of gram positive bacteria a rigid structure which creates difficulty for silver nanoparticles to penetrate the bacterial cell wall [72]. In Gram negative bacteria the cell wall possesses thinner peptidoglycan layer, due to which silver nanoparticles could easily release silver ion causing damage to membrane leading to bactericidal activity [85]. It has been reported earlier that silver nanoparticles prepared with extract of *Aloe vera* [86], *Eriobotrya japonica* [87], *Sida acuta* [88], *Capparis spinosa* [89], *Lycopersicon esculentum* [90], *Artocarpus heterophyllum* [67] showed strong antimicrobial activity against different strains of microorganisms.

On assessing MIC value of silver nanoparticles against different tested microorganisms (Fig. 12) it was found that silver nanoparticles showed highest bactericidal activity against gram negative bacteria, *S. typhimurium* followed by *Escherichia coli* with MIC value of 40 µg/ml and 60 µg/ml respectively. The MIC value of gram positive bacteria was found to be on higher site with maximum value of 160 µg/ml in *Bacillus megaterium*. MIC value against gram negative bacteria appeared at low nanosilver concentration probably because the thin peptidoglycan layer of gram negative

Table 1 Variation in crystalline size, dislocation density, inter planar spacing, lattice constant and cell volume of synthesized nanoparticles

2θ	Orientation	Intensity	FWHM (°)	D (nm)	δ (nm ⁻²)	d (Å)	a ₀ (Å)	Cell volume (Å ³)
38.14	111	393.44	0.7887	10.6567	0.0088	2.358	4.084	68.096
44.26	200	79.12	1.0685	8.0258	0.0155	2.045	4.090	68.399
64.46	220	116.06	0.6677	14.0642	0.0051	1.444	4.085	68.179
77.41	311	93.25	1.3229	7.6951	0.0169	1.232	4.086	68.199

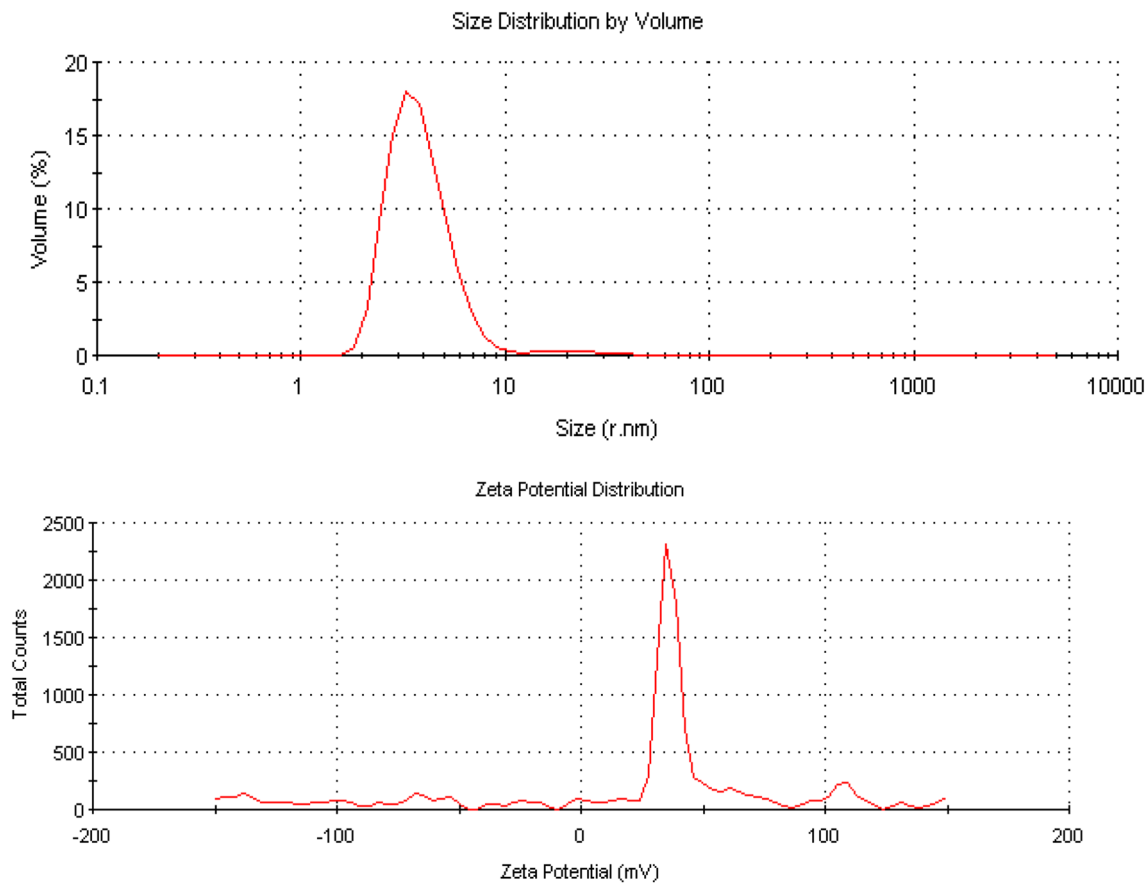


Fig. 10 DLS size distribution pattern and zeta potential of biosynthesized silver nanoparticles using mulberry leaf extract

bacteria easily permits nanoparticles to penetrate the cell wall [91]. Silver nanoparticles by releasing silver cations inhibit bacterial growth by damaging cellular organization [92]. Stoimenov et al. [93] reported that electrostatic force of attraction between positively charged nanoparticles and negatively charged microbial membrane was the driving force for bactericidal activity. Silver nanoparticles by interacting with negatively charged phosphorous and sulphur containing cellular constituents like DNA and proteins inhibit microbial growth [94, 95]. Although in recent years different mode of action of silver nanoparticles has been demonstrated by different workers but exact mode of action was not clear and requires further analysis.

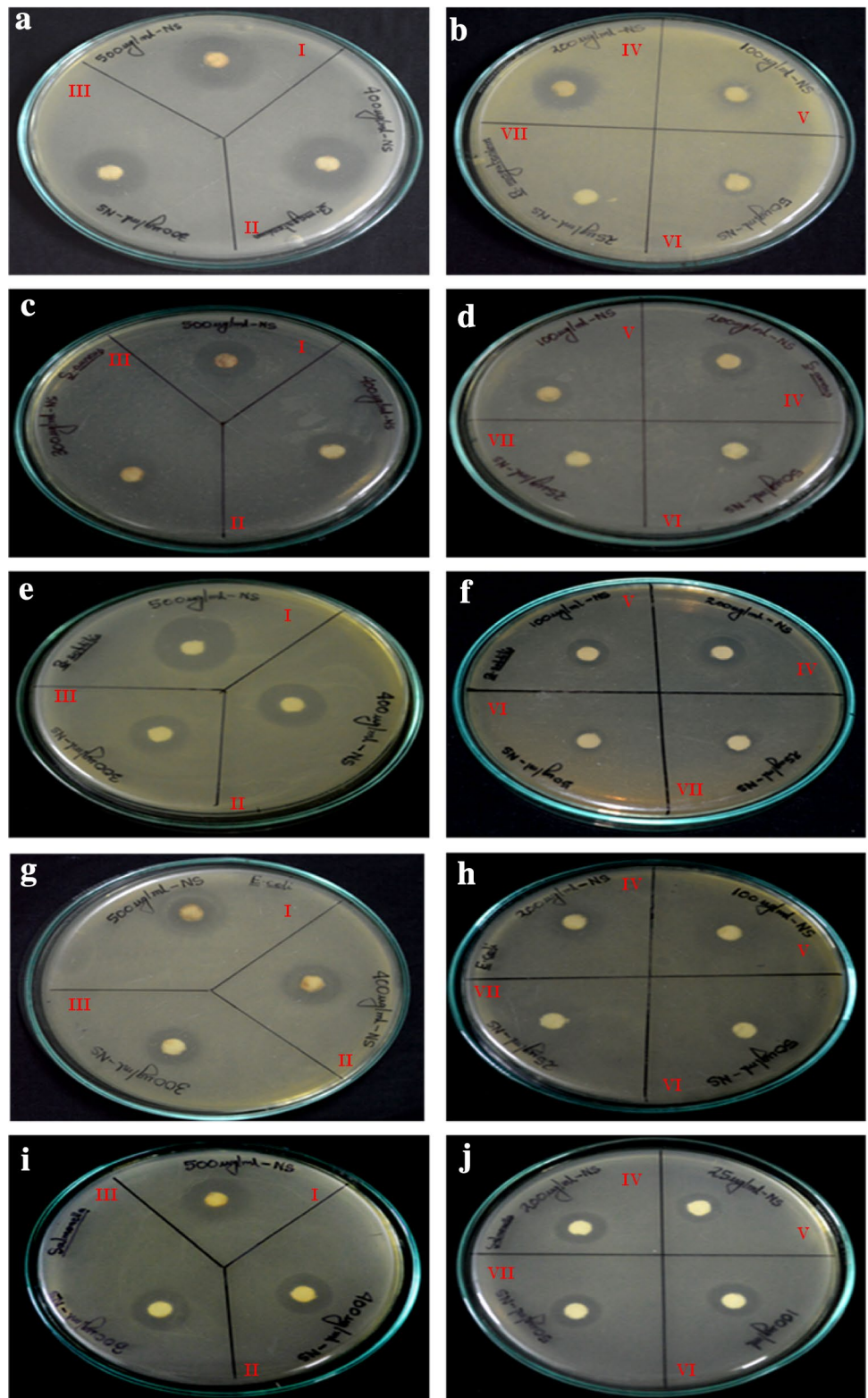
3.9 Antioxidant activity

Biosynthesized silver nanoparticles exhibit significant dose dependent scavenging activity against all the free radicals as shown in Fig. 13. The functional groups of leaf extract that are involved in reduction of silver ion for nanosilver formation are mainly responsible for its antioxidant activity [96].

The lipophilic radical DPPH was considered as model test for determining the free radical scavenging activity of synthesized nanoparticles and natural compounds because of its high stability [97]. In its radical form, DPPH shows maximum absorbance at 517 nm which gradually decreases by reduction caused by antioxidants [98]. In present study DPPH scavenging activity increases with increase in concentration of synthesized nanoparticles with maximum activity of 47.81% at highest concentration (100 $\mu\text{g/ml}$) which is $\sim 56\%$ of the activity showed by standard ascorbic acid at the same concentration, while plant extract showed considerably less scavenging activity of 36.22%. Our finding in the present study was supported by earlier workers who also observed almost similar outcome while working with silver nanoparticles prepared using extract of *Iresine herbstii* [99], *Alpinia katsumadai* [100].

ABTS scavenging activity of silver nanoparticles was evaluated using BTH as standard. Oxidation of ABTS with potassium persulfate generates ABTS^+ cation, a blue chromophore that causes oxidative damage [27]. ABTS^+ scavenging activity is mostly used to access the potential of hydrogen donors and antioxidant agents present in

Fig. 11 Antimicrobial activity of silver nanoparticles at seven different concentrations (I—500, II—400, III—300, IV—200, V—100, VI—50, VII—25 µg/ml) against **a, b** *Bacillus megaterium*, **c, d** *Staphylococcus aureus*, **e, f** *Bacillus subtilis*, **g, h** *Escherichia coli*, **i, j** *Salmonella typhimurium*



the biological samples [26]. Silver nanoparticles displayed maximum ABTS⁺ scavenging activity of 95.08% almost equivalent to that exhibited by BTH standard 95.51% at 100 µg/ml, representing strong activity. Strong ABTS⁺

scavenging activity of green synthesized silver nanoparticles was also reported by Shanmugam et al. [101].

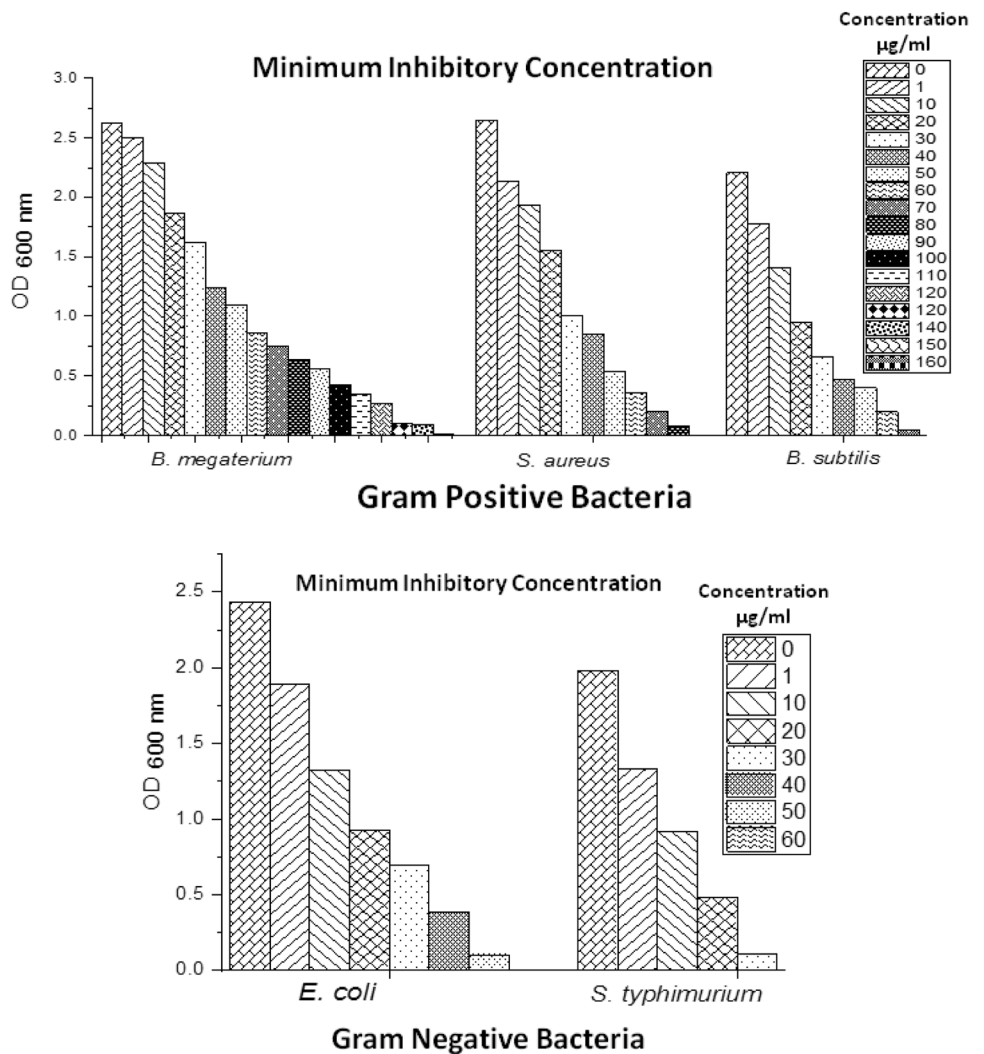
Silver nanoparticles showed 64.04% nitric oxide scavenging activity at 100 µg/ml in comparison with

Table 2 Antimicrobial activity of silver nanoparticles against tested microorganisms

Microorganism	Zone of inhibition (mm)						
	500 µg/ml	400 µg/ml	300 µg/ml	200 µg/ml	100 µg/ml	50 µg/ml	25 µg/ml
<i>Bacillus megaterium</i>	22.03 ± 1.06 ^a	20.00 ± 0.78 ^{ab}	18.31 ± 1.02 ^{bc}	16.95 ± 1.55 ^c	11.19 ± 1.02 ^d	9.32 ± 1.28 ^{de}	6.61 ± 1.53 ^e
<i>Staphylococcus aureus</i>	16.61 ± 1.06 ^a	15.08 ± 0.78 ^{ab}	13.73 ± 0.88 ^{bc}	12.71 ± 0.51 ^{cd}	11.36 ± 1.28 ^{de}	10.17 ± 1.35 ^e	7.10 ± 1.02 ^f
<i>Bacillus subtilis</i>	21.86 ± 1.02 ^a	17.97 ± 0.78 ^b	15.93 ± 0.59 ^c	11.86 ± 1.28 ^d	11.36 ± 1.06 ^d	9.15 ± 1.02 ^e	7.29 ± 0.29 ^e
<i>Escherichia coli</i>	20.51 ± 1.06 ^a	19.49 ± 1.55 ^a	15.93 ± 0.78 ^b	11.53 ± 1.28 ^c	10.17 ± 1.35 ^{cd}	8.64 ± 1.02 ^{de}	7.12 ± 1.02 ^e
<i>Salmonella typhimurium</i>	17.97 ± 1.28 ^a	16.27 ± 0.51 ^{ab}	15.42 ± 1.06 ^{bc}	13.90 ± 0.78 ^{cd}	13.39 ± 1.06 ^{cd}	12.54 ± 0.78 ^{de}	10.51 ± 1.17 ^e

Results are expressed as Mean ± SEM of triplicate determinations. Values with different letters (a, b, c, etc.) differ significantly ($p \leq 0.05$) by Duncan’s Multiple Range Test

Fig. 12 Minimum inhibitory concentration of silver nanoparticles against tested microorganisms



88.62% and 45.72% in gallic acid standard and plant extract respectively. Silver nanoparticles utilize electron-generative property of nitric oxide radical for reducing by donating electron [102]. Nitric oxide plays vital role in bio-regulation, but excess production or accumulation of nitric oxide may cause several disorders [96]. Silver

nanoparticles through its scavenging potential nullify the harmful effect of nitric oxide.

Superoxide scavenging activity was measured at 560 nm and reduction in absorption value indicates consumption of superoxide ions by antioxidants. Silver nanoparticles at 100 µg/ml concentration exhibit

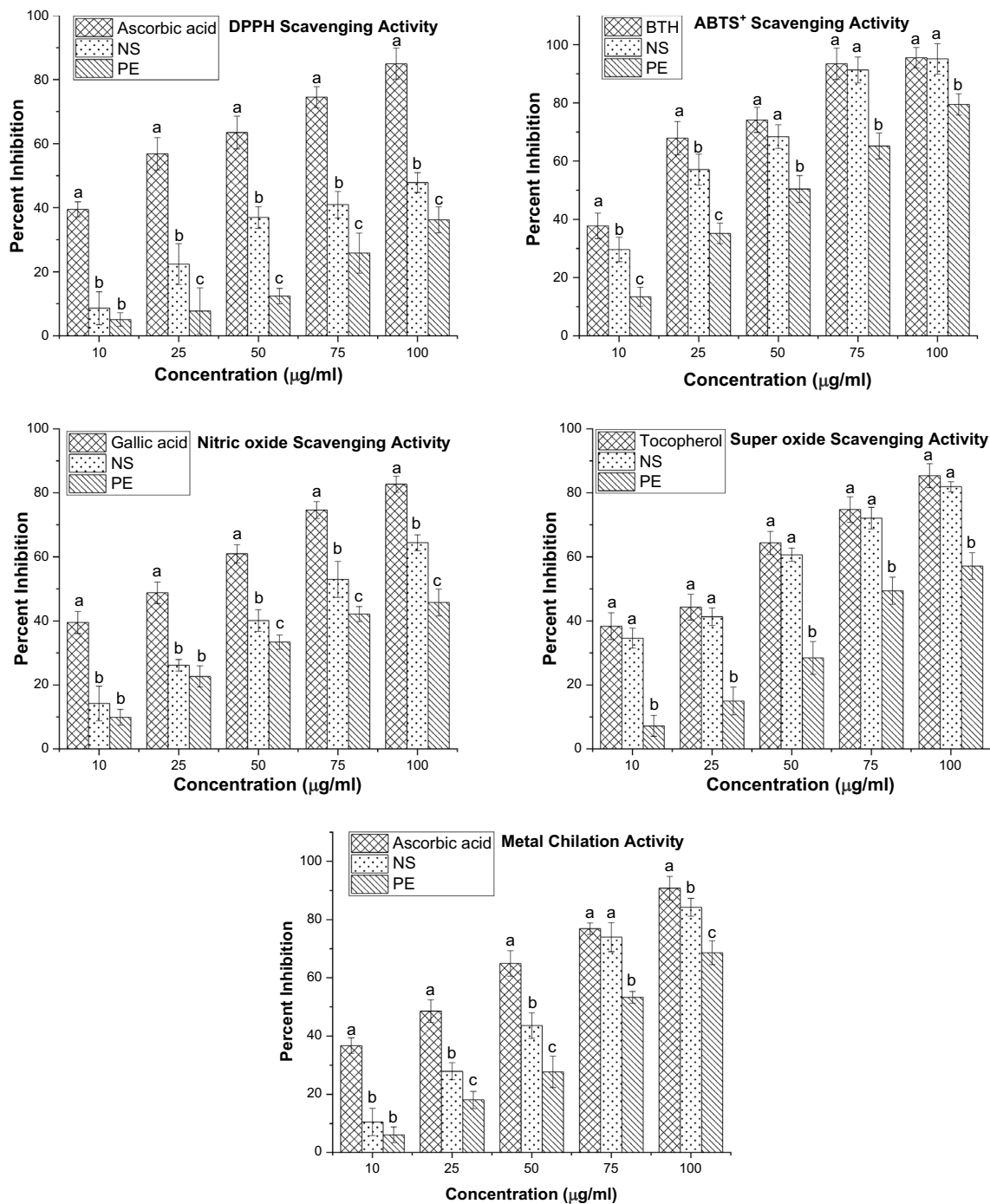


Fig. 13 DPPH, ABTS, nitric oxide, super oxide and metal chelating scavenging activity of biosynthesized silver nanoparticles in comparison with plant extract and respective standards (results are

expressed as mean ± STDEV of triplicate determinations. Values with different letters (a, b, c, etc.) differ significantly ($p \leq 0.05$) by Duncan's multiple range test)

significant superoxide scavenging activity of 81.92% in comparison with 85.35% in tocopherol standard. Superoxide is a weak anionic radical but bears the capacity to generate two harmful radicals, hydroxyl radical and singlet oxygen that develops oxidative stress [103]. Inside living system superoxide directly reacts and damages

DNA and protein [104], besides this hydroxyl radical generated by superoxide causes cellular damage by reacting with polyunsaturated fatty acid associated with phospholipids [105]. In present study silver nanoparticles showed high superoxide scavenging activity which was supported by Reddy et al. [104] showing 60% superoxide

Table 3 IC₅₀ value of silver nanoparticles, plant extract with respect to standards

Antioxidant	IC ₅₀ (µg/ml)		
	Standard	Nano silver	Plant extract
DPPH	20.744	97.273	143.967
ABTS	12.016	25.929	53.832
Superoxide	30.895	37.097	77.479
Nitric oxide	28.685	70.992	101.587
Metal chelation	28.999	54.325	73.837

scavenging with silver nanoparticles prepared using fruit extract of *Piper longum*.

Metal chelating is the ability of the antioxidant to destabilize the formation of Ferrozine-Fe²⁺ complex [106]. Metal chelating activity was estimated at 562 nm and decrease in absorption in respect to control indicates the ability of antioxidant to bind with iron. Nanosilver at 100 µg/ml concentration exhibits 84.24% metal chelation, while at same concentration plant extract and ascorbic acid standard showed 68.62% and 90.81% scavenging activity respectively, indicating high metal chelation potential of biosynthesized nano particles with respect to standard.

IC₅₀ value of synthesized silver nano particles, plant extract and respective standards against all the studied antioxidants are enlisted in Table 3. It was observed that silver nanoparticles showed maximum activity against ABTS⁺ cation radical with IC₅₀ of 25.929 µg/ml, while least activity was against DPPH scavenging activity having IC₅₀ of 97.27 µg/ml. In comparison with standard, it can be stated that IC₅₀ of synthesized nanoparticles increased significantly with respect to plant extract from which it was prepared.

4 Conclusion

Mulberry leaves as an agricultural product in the field of sericulture has been successfully utilized for quick, simple, stable, eco-friendly and cost-effective production of silver nanoparticles using biogenic process. UV-visible spectral analysis reveals that the optimum concentration for nanosilver formation is 10⁻³ M silver nitrate and 5 ml plant extract. The synthesized nanoparticles were crystalline and spherical in nature with average particle size ranges from 10 to 16 nm as revealed through XRD, SEM and TEM analysis. FTIR analysis showed that the stability of silver nanoparticles was mainly due to the presence of proteins, carbohydrate and different secondary metabolites that acts as reducing and capping agents. Synthesized nanoparticles showed high potential to protect against damage caused by free

radicals. The antimicrobial screening demonstrates that biosynthesized silver nanoparticles exhibit strong antimicrobial activity against both gram positive and gram negative microorganisms. From our study it may be recommended that synthesized silver nanoparticles can be explored as an alternative option in the prevention of diseases related with generation of free radicals and also in reducing microbial count in biological systems.

Acknowledgements The first author would like to thank University Grants Commission for financial assistance (Grant No. 365932), as the author receives UGC-NET JRF Fellowship. The authors would like to thank Directorate of Textiles (Sericulture), Matigara Sericulture Complex for providing necessary mulberry leaves during experiment. The author would also like to thank SAIF, IIT Bombay and SAIF, Cochin University of Science and Technology for assisting while conducting different instrument analysis.

Compliance with ethical standards

Conflict of interest The author report no conflicts of interest. The work was purely conducted for research purpose only.

References

- Kuppurangan G, Karupphasamy B, Nagarajan K, Sekar RK, Viswaprakash N, Ramasamy T (2016) Biogenic synthesis and spectroscopic characterization of silver nanoparticles using leaf extract of *Indoneesiella echioides*: in vitro assessment on antioxidant, antimicrobial and cytotoxicity potential. *Appl Nanosci* 6:973–982
- Larue C, Castillo-Michel H, Sobanska S, Cecillon L, Bureau S, Barthes V et al (2014) Foliar exposure of the crop *Lactuca sativa* to silver nanoparticles: evidence for internalization and changes in Ag speciation. *J Hazard Mater* 264:98–106
- Awwad AM, Salem NM, Abdeen AO (2013) Green synthesis of silver nanoparticles using carob leaf extract and its antibacterial activity. *Int J Ind Chem* 4(29):1–6
- Tolaymat TM, Badawy AM, Genaidy A, Scheckel KG, Luxton TP, Suidan M (2010) An evidence-based environmental perspective of manufactured silver nanoparticles in syntheses and applications: a systematic review and critical appraisal of peer-reviewed scientific papers. *Sci Total Environ* 408(5):999–1006
- Liz-Marzán LM, Lado-Touriño I (1996) Reduction and stabilization of silver nanoparticles in ethanol by non-ionic surfactants. *Langmuir* 12:3585–3589
- Adner D, Noll J, Schulze S, Hietschold M, Lang H (2016) Aspherical silver nanoparticles by thermal decomposition of a single-source-precursor. *Inorg Chim Acta* 446:19–23. <https://doi.org/10.1016/j.ica.2016.02.059>
- Akhbari K, Morsali A, Retailleau P (2010) Silver nanoparticles from the thermal decomposition of a two-dimensional nano-coordination polymer. *Polyhedron* 29(18):3304–3309
- Park HH, Zhang X, Choi YJ, Hill RH (2011) Synthesis of Ag nanostructures by photochemical reduction using citrate-capped pt seeds. *J. Nanomater.* <https://doi.org/10.1155/2011/265287>
- Bae CH, Nam SH, Park SM (2002) Formation of silver nanoparticles by laser ablation of silver target in NaCl solutions. *Appl Surf Sci.* [https://doi.org/10.1016/S0169-4332\(02\)00430-0](https://doi.org/10.1016/S0169-4332(02)00430-0)

10. Nadagouda MN, Speth TF, Varma RS (2011) Microwave-assisted green synthesis of silver nanostructures. *Acc Chem Res* 44(7):469–478
11. Sunkar S, Nachiyar CV (2012) Biogenesis of antibacterial silver nanoparticles using the endophytic bacterium *Bacillus cereus* isolated from *Garcinia xanthochymus*. *Asian Pac J Trop Biomed* 2(12):953–959
12. Das VL, Thomas R, Varghese RT, Soniya EV, Mathew J, Radhakrishnan EK (2014) Extracellular synthesis of silver nanoparticles by the *Bacillus* strain CS 11 isolated from industrialized area. *Biotech* 4:121–126. <https://doi.org/10.1007/s13205-013-0130-8>
13. Vigneshwaran N, Ashtaputre NM, Varadarajan PV, Nachane RP, Paralikar KM, Balasubramanya RH (2007) Biological synthesis of silver nanoparticles using the fungus *Aspergillus flavus*. *Mater Lett* 61:1413–1418
14. Shaik MR, Khan M, Kuniyil M, Al-Warthan A, Alkathlan HZ, Siddiqui MR, Shaik JP, Ahamed A, Mahmood A, Khan M, Adil SF (2018) Plant-extract-assisted green synthesis of silver nanoparticles using *Origanum vulgare* L. extract and their microbicidal activities. *Sustainability* 10:913. <https://doi.org/10.3390/su10040913>
15. Rajagopal T, Jemimah IA, Ponmanickam P, Ayyanar M (2015) Synthesis of silver nanoparticles using *Catharanthus roseus* root extract and its larvicidal effects. *J Environ Biol* 36(6):1283–1289
16. Ali ZA, Yahya R, Sekaran SD, Puteh R (2016) Green synthesis of silver nanoparticles using apple extract and its antibacterial properties. *Adv Mater Sci Eng.* <https://doi.org/10.1155/2016/4102196>
17. Jaina D, Daimab HK, Kachhwahaa S, Kothari SL (2009) Synthesis of plant-mediated silver nanoparticles using papaya fruit extract and evaluation of their anti microbial activities. *Dig J Nanomater Biostruct* 4(4):723–727
18. Patil SV, Borase HP, Patil CD, Salunke BK (2012) Biosynthesis of silver nanoparticles using latex from few Euphorbian plants and their antimicrobial potential. *Appl Biochem Biotechnol* 167(4):776–790. <https://doi.org/10.1007/s12010-012-9710-z>
19. Talekar S, Joshi A, Chougale R, Nakhe A, Bhojwani R (2016) Immobilized enzyme mediated synthesis of silver nanoparticles using cross-linked enzyme aggregates (CLEAs) of NADH-dependent nitrate reductase. *Nano-Struct Nano-Objects* 6:23–33
20. Hamedi S, Ghaseminezhad M, Shokrollahzadeh S, Shojaosadati SA (2016) Controlled biosynthesis of silver nanoparticles using nitrate reductase enzyme induction of filamentous fungus and their antibacterial evaluation. *Artif Cells Nanomed Biotechnol.* <https://doi.org/10.1080/21691401.2016.1267011>
21. Mishra A, Sarda M (2012) Alpha-amylase mediated synthesis of silver nanoparticles. *Sci Adv* 4:143–146
22. Ahmed S, Ahmad M, Swami BL, Ikram S (2016) A review on plants extract mediated synthesis of silver nanoparticles for antimicrobial applications: a green expertise. *J Adv Res* 7(1):17–28
23. Ahmed S, Saifukkah Ahmad M, Swami BL, Ikram S (2015) Green Synthesis of silver nanoparticles using *Azadirachta indica* aqueous leaf extract. *J Radiat Res Appl Sci* 9:1–7
24. Gomathi M, Rajkumar PV, Prakasam A, Ravichandran K (2017) Green synthesis of silver nanoparticles using *Datura stramonium* leaf extract and assessment of their antibacterial activity. *Resource Efficient Technol* 3:280–284
25. Mitiku AA, Yilma B (2017) Antibacterial and antioxidant activity of silver nanoparticles synthesized using aqueous extract of *Moringa stenopetala* leaves. *Afr J Biotechnol* 16(32):1705–1716. <https://doi.org/10.5897/ajb2017.16010>
26. Ajayi E, Afolayan A (2017) Green synthesis, characterization and biological activities of silver nanoparticles from alkalized *Cymbopogon citratus* Stapf. *Adv Nat Sci Nanosci.* <https://doi.org/10.1088/2043-6254/aa5cf7>
27. Moteriya P, Padalia H, Chanda S (2017) Characterization, synergistic antibacterial and free radical scavenging efficacy of silver nanoparticles synthesized using *Cassia roxburghii* leaf extract. *J Gen Eng Biotech* 15:505–513
28. Phull AR, Abbas Q, Ali A, Raza H, Kim SJ, Zia M, Haq I (2016) Antioxidant, cytotoxic and antimicrobial activities of green synthesized silver nanoparticles from crude extract of *Bergeia ciliate*. *Future J Pharma Sci* 2:31–36
29. Sundararajan B, Mahendran G, Thamaraiselvi R, Ranjitha Kumari BD (2016) Biological activities of synthesized silver nanoparticles from *Cardiospermum halicacabum* L. *Bull Mater Sci* 39(2):423–431
30. Banala RR, Nagati VB, Karnati PR (2015) Green synthesis and characterization of *Carica papaya* leaf extract coated silver nanoparticles through X-ray diffraction, electron microscopy and evaluation of bactericidal properties. *Saudi J Biol Sci* 22:637–644
31. Premasudha P, Venkataramana M, Abirami M, Vanathi P, Krishna K, Rajendran R (2015) Biological synthesis and characterization of silver nanoparticles using *Eclipta alba* leaf extract and evaluation of its cytotoxic and antimicrobial Potential. *Bull Mater Sci* 38(4):965–973
32. Tikader A, Vijayan K (2010) Assessment of biodiversity and strategies for conservation of genetic resources in mulberry (*Morus* spp.). *Bioremediat Biodivers Bioavail* 4(Special Issue 1):15–27
33. Lee SH, Choi SY, Kim H, Hwang JS, Lee BG, Gao JJ (2002) Mulberrosin F isolated from the leaves of *Morus alba* inhibits melanin biosynthesis. *Biol Pharm Bull* 25:1045–1048
34. Sohn HY, Son KH, Kwon CS, Kwon GS, Kang SS (2004) Antimicrobial and cytotoxic activity of 18 prenylated flavonoids isolated from medicinal plants: *Morus alba* L., *Morus mongolica* Schneider., *Broussonetia papyrifera* (L.) Vent, *Sophora flavescens* Ait and *Echinosophora koreensis* Nakai. *Phytomedicine* 11:666–672
35. Wattanapitayakul SK, Chularojmontri L, Herunsalee A, Charuchongkolwongse S, Niumsukul S, Bauer JA (2005) Screening of antioxidants from medicinal plants for cardioprotective effect against doxorubicin toxicity. *Basic Clin Pharmacol Toxicol* 96:80–87
36. Oh H, Ko EK, Jun JY, Oh MH, Park SU, Kang KH, Lee HS, Kim YC (2002) Hepatoprotective and free radical scavenging activities of prenylflavonoids coumarin and stilbene from *Morus alba*. *Planta Med* 68:932–934
37. Niidome T, Takahashi K, Goto Y, Goh SM, Tanaka N, Kamei K (2007) Mulberry leaf extract prevents amyloid beta-peptide fibril formation and neurotoxicity. *NeuroReport* 18:813–816
38. Kofujita H, Yaguchi M, Doi N, Suzuki K (2004) A novel cytotoxic prenylated flavonoid from the root of *Morus alba*. *J Insect Biotechnol Sericol* 73:113–116
39. Hogade MG, Patil KS, Wadkar GH, Mathapati SS, Dhupal PB (2010) Hepatoprotective activity of *Morus alba* (Linn.) leaves extract against carbon tetrachloride induced hepatotoxicity in rats. *Afr J Pharm Pharmacol* 4(10):731–734
40. Thaipitakwong T, Numhomb S, Aramwit P (2018) Mulberry leaves and their potential effects against cardiometabolic risks: a review of chemical compositions, biological properties and clinical efficacy. *Pharm Biol* 56(1):109–118. <https://doi.org/10.1080/13880209.2018.1424210>
41. Wilson RD, Islam MS (2015) effects of white mulberry (*Morus alba*) leaf tea investigated in a type 2 diabetes model of rats. *Acta Pol Pharm* 72(1):153–160
42. Awwad AM, Salem NM (2012) Green synthesis of silver nanoparticles by mulberry leaf extract. *J Nanosci Nanotechnol* 2(4):125–128

43. Singh A, Dar MY, Joshi B, Sharma B, Shrivastava S, Shukla S (2018) Phytofabrication of silver nanoparticles: novel drug to overcome hepatocellular ailments. *Toxicol Rep* 5:333–342
44. Akbal A, Turkdemir MH, Cicek A, Ulug B (2016) Relation between silver nanoparticle formation rate and antioxidant capacity of aqueous plant leaf extracts. *J Spectrosc*. <https://doi.org/10.1155/2016/4083421>
45. Li XC, Wu XT, Huang L (2009) Correlation between antioxidant activities and phenolic contents of radix *Angelicae sinensis* (Danggui). *Molecules* 14:5349–5361
46. Sidduraju P, Mohan P, Becker K (2002) Studies on the antioxidant activity of Indian *Laburnum Cassia fistula* L: a preliminary assessment of crude extracts from stem bark, leaves, flowers and fruit pulp. *Food Chem* 79:61–67
47. Fu W, Chen J, Cai Y, Lei Y, Chen L, Pei L, Zhou D, Liang X, Ruan J (2010) Antioxidant, free radical scavenging, anti-inflammatory and hepatoprotective potential of the extract from *Parathelypteris nipponica* (Franch. Et Sav.) Ching. *J Ethnopharmacol* 130:521–528
48. Marcocci L, Packer L, Droy-Lefaix MT, Sekaki A, Grades-Albert M (1994) Antioxidant action of *Ginkgo biloba* extracts EGb 761. *Methods Enzymol* 234:462–475
49. Dinis TCP, Madeira VM, Almeida LM (1994) Action of phenolic derivatives (acetaminophen, salicylate and 5-aminosalicylate) as inhibitors of membrane lipid peroxidation and as peroxyl radical scavengers. *Arch Biochem Biophys* 315(1):161–169
50. Annamalai A, Christina VLP, Christina V, Lakshmi PTV (2014) Green synthesis and characterisation of Ag NPs using aqueous extract of *Phyllanthus maderaspatensis* L. *J Exp Nanosci* 9(2):113–119
51. Sastry M, Mayya KS, Bandyopadhyay K (1997) pH dependent changes in the optical properties of carboxylic acid derivatized silver colloidal particles. *Colloids Surf A* 127:221–228
52. Shankar T, Karthiga P, Swarnalatha K, Rajkumar K (2017) Green synthesis of silver nanoparticles using *Capsicum frutescens* and its intensified activity against *E. coli*. *Resource Efficient Technol* 3:303–308
53. Bar H, Bhui DK, Sahoo GP, Sarkar P, Sarkar PD, Misra A (2009) Green synthesis of silver nanoparticles using latex of *Jatropha curcas*. *Colloids Surf A Physiochem Eng Asp* 339:134–139
54. Balavijayalakshmi J, Ramalakshmi V (2017) Carica papaya peel mediated synthesis of silver nanoparticles and its antibacterial activity against human pathogens. *J Appl Res Technol* 15:413–422
55. Kaya H, Aydin F, Gürkan M, Yılmaz S, Ates M, Demir V, Arslan Z (2016) A comparative toxicity study between small and large size zinc oxide nanoparticles in tilapia (*Oreochromis niloticus*): organ pathologies, osmoregulatory responses and immunological parameters. *Chemosphere* 144:571–582
56. Bhakya S, Muthukrishnan S, Sukumaran M, Muthukumar M (2016) Biogenic synthesis of silver nanoparticles and their antioxidant and antibacterial activity. *Appl Nanosci* 6:755–766. <https://doi.org/10.1007/s13204-015-0473-z>
57. Ganesh Babu MM, Gunasekaran P (2009) Production and structural characterization of crystalline silver nanoparticles from *Bacillus cereus* isolate. *Colloids Surf B Biointerfaces* 74:191–195
58. Loo YY, Chieng BW, Nishibuchi M, Radu S (2012) Synthesis of silver nanoparticles by using tea leaf extract from *Camellia sinensis*. *Int J Nanomed* 7:4263–4267
59. Khalil MMH, Ismail EH, El-Baghdady KZ, Mohamed D (2014) Green synthesis of silver nanoparticles using olive leaf extract and its antibacterial activity. *Arab J Chem* 7(6):1131–1139
60. Sivakumar P, Nethradevi C, Renganathan S (2012) Synthesis of silver nanoparticles using *Lantana camara* fruit extract and its effect on pathogens. *Asian J Pharm Clin Res* 5(3):97–101
61. Gurunathan S, Jeong JK, Han JW, Zhang XF, Park JH, Kim JH (2015) Multidimensional effects of biologically synthesized silver nanoparticles in *Helicobacter pylori*, *Helicobacter felis*, and human lung (L132) and lung carcinoma A549 cells. *Nanoscale Res Lett*. <https://doi.org/10.1186/s11671-015-0747-0>
62. Yuen CWM, Ku SKA, Choi PSR, Kan CW, Tsang SY (2005) Determining functional groups of commercially available ink-jet printing reactive dyes using infrared spectroscopy. *Res J Text Apparel* 9(2):26–38
63. Shankar SS, Rai A, Absar Ahmad A, Sastry M (2004) Rapid synthesis of Au, Ag, and bimetallic Au core–Ag shell nanoparticles using neem (*Azadirachta indica*) leaf broth. *J Coll Interface Sci* 275:496–502
64. Butt MS, Nazir A, Sultan MT, Schroën K (2008) *Morus alba* L. nature's functional tonic. *Trends Food Sci Technol* 19:505–512
65. Liang Q, Wang Q, Wang Y, Wang Y, Hao J, Jiang M (2018) Quantitative ¹H-NMR spectroscopy for profiling primary metabolites in mulberry leaves. *Molecules*. <https://doi.org/10.3390/molecules23030554>
66. Hunyadi A, Liktör-Busa E, Márki Á, Martins A, Jedlinszki N, Hsieh TJ, Báthori M, Hohmann J, Zupkó I (2013) Metabolic effects of mulberry leaves: exploring potential benefits in type 2 diabetes and hyperuricemia. *J Evid Based Complement Altern Med*. <https://doi.org/10.1155/2013/948627>
67. Jagtap UB, Bapat VA (2013) Green synthesis of silver nanoparticles using *Artocarpus heterophyllus* Lam. seed extract and its antibacterial activity. *Ind Crops Prod* 46(2013):132–137
68. Magudapatty P, Gangopadhyayans P, Panigrahi BK, Nair KGM, Dhara S (2001) Electrical transport studies of Ag nanoclusters embedded in glass matrix. *Phys B* 299:142–146
69. Das J, Das MP, Velusamy P (2013) *Sesbania grandiflora* leaf extract mediated green synthesis of antibacterial silver nanoparticles against selected human pathogens. *Spectrochim Acta A Mol Biomol Spectrosc* 104:265–270
70. Puchalski M, Dąbrowski P, Olejniczak W, Krukowski P, Kowalczyk P, Polański K (2007) The study of silver nanoparticles by scanning electron microscopy, energy dispersive X-ray analysis and scanning tunnelling microscopy. *Mater Sci Pol* 25(2):473–478
71. Ahmad N, Sharma S, Alam MK, Singh VN, Shamsi SF, Mehta BR, Fatma A (2010) Rapid synthesis of silver nanoparticles using dried medicinal plant of basil. *Colloids Surf B* 81:81–86
72. Ibrahim HMM (2015) Green synthesis and characterization of silver nanoparticles using banana peel extract and their antimicrobial activity against representative microorganisms. *J Radiat Res Appl Sci* 8:265–275
73. Bansal V, Li V, O'Mullane AP, Bhargava SK (2010) Shape dependent electrocatalytic behaviour of silver nanoparticles. *CrystEngComm* 12(12):4280–4286
74. Agnihotri S, Mukherji S, Mukherji S (2014) Size-controlled silver nanoparticles synthesized over the range 5–100 nm using the same protocol and their antibacterial efficacy. *RSC Adv* 4:3974–3983
75. Roopan SM, Rohit Madhumitha G, Rahuman AA, Kamaraj C, Bharathi A, Surendra TV (2013) Low-cost and ecofriendly phyto-synthesis of silver nanoparticles using *Cocos nucifera* coir extract and its larvicidal activity. *Ind Crops Prod* 43:631–635
76. Amin M, Anwar F, Janjua MRSA, Iqbal MA, Rashid U (2012) Green synthesis of silver nanoparticles through reduction with *Solanum xanthocarpum* L. berry extract: characterization, antimicrobial and urease inhibitory activities against *Helicobacter pylori*. *Int J Mol Sci* 13:9923–9941. <https://doi.org/10.3390/ijms13089923>
77. Anandalakshmi K, Venugopal J, Ramasamy V (2016) Characterization of silver nanoparticles by green synthesis method using *Petalium murex* leaf extract and their antibacterial

- activity. *Appl Nanosci* 6:399–408. <https://doi.org/10.1007/s13204-015-0449-z>
78. Mehta BK, Chhajlani M, Shrivastava BD (2017) Green synthesis of silver nanoparticles and their characterization by XRD. *J Phys: Conf Ser*. <https://doi.org/10.1088/1742-6596/836/1/012050>
 79. Singhal G, Bhavesh R, Kasariya K, Sharma AR, Singh RP (2011) Biosynthesis of silver nanoparticles using *Ocimum sanctum* (Tulsi) leaf extract and screening its antimicrobial activity. *J Nanopart Res* 13:2981–2988
 80. Aiad I, El-Sukkary MM, Soliman EA, El-Awady MY, Shaban SM (2013) In situ and green synthesis of silver nanoparticles and their biological activity. *J Ind Eng Chem* 1:2. <https://doi.org/10.1016/j.jiec.2013.12.031>
 81. Haider Mohammed J, Mehdi MS (2014) Study of morphology and zeta potential analyzer for the silver nanoparticles. *Int J Sci Eng Res* 5(7):381–385
 82. Zhang Y, Yang M, Portney NG, Cui D, Budak G, Ozbay E, Ozkan M, Ozkan CS (2008) Zeta Potential: a surface electrical characteristic to probe the interaction of nanoparticles with normal and cancer human breast epithelial cell. *Biomed Microdevices* 10:321–328
 83. Hedberg J, Lundin M, Lowe T, Blomberg E, Wold S, Wallinder IO (2012) Interactions between surfactants and silver nanoparticles of varying charge. *J Colloid Interface Sci* 369:193–201
 84. Beveridge TJ, Fyfe WS (1985) Metal fixation by bacterial cell walls. *Can J Earth Sci* 22:1893–1898
 85. Flores-López NS, Cortez-Valadez M, Moreno-Ibarra GM, Larios-Rodríguez E, Torres-Flores EI, Delgado-Beleño Y, Martínez-Núñez CE, Ramírez-Rodríguez LP, Arizpe-Chávez H, Castro-Rosas J, Ramírez-Bon R, Flores-Acosta M (2016) Silver nanoparticles and silver ions stabilized in NaCl nanocrystals. *Physica E* 84:482–488. <https://doi.org/10.1016/j.physe.2016.07.012>
 86. Abalkhila TA, Alharbia SA, Salmeha SH, Wainwright M (2017) Bactericidal activity of biosynthesized silver nanoparticles against human pathogenic bacteria. *Biotechnol Biotechnol Equip* 31(2):411–417. <https://doi.org/10.1080/13102818.2016.1267594>
 87. Rao B, Tang RC (2017) Green synthesis of silver nanoparticles with antibacterial activities using aqueous *Eriobotrya japonica* leaf extract. *Adv Nat Sci Nanosci Nanotechnol* 8(1):1–8
 88. Nisha C, Bhawana P, Fulekar MH (2017) Antimicrobial potential of green synthesized silver nanoparticles using *Sida acuta* leaf extract. *Nano Sci Nano Technol* 11(1):111–119
 89. Benakashani F, Allafchian AR, Jalali SAH (2016) Biosynthesis of silver nanoparticles using *Capparis spinosa* L. leaf extract and their antibacterial activity. *Karbala Int J Mod Sci* 2:251–258
 90. Maiti S, Krishnan D, Barman G, Ghosh SK, Laha JK (2014) Antimicrobial activities of silver nanoparticles synthesized from *Lycopersicon esculentum* extract. *J Anal Sci Technol* 5(40):1–7
 91. Shrivastava S, Bera T, Roy A, Singh G, Ramachandrarao P, Dash D (2007) Characterization of enhanced antibacterial effects of novel silver nanoparticles. *Nanotechnology* 18:103–112
 92. Paszek E, Czyz J, Woznicka O, Jakubiak D, Woźnicka J, Łojkowski W, Stepień E (2012) Zinc oxide nanoparticles impair the integrity of human umbilical vein endothelial cell monolayer in vitro. *J Biomed Nanotechnol* 8(6):957–967
 93. Stoimenov PK, Klinger RL, Marchin GL, Klabunde KJ (2000) Metal oxide nanoparticles as bactericidal agents. *Langmuir* 18:6679–6686
 94. Nel AE, Mädler L, Velegol D, Xia T, Hoek EMV, Somasundaran P, Klaessig F, Castranova V, Thompson M (2009) Understanding bio physicochemical interactions at the nano-bio interface. *Nat Mater* 8:543–557
 95. Jung W, Koo H, Kim K, Shin S, Kim S, Park Y (2008) Antibacterial activity and mechanism of action of the silver ion in *Staphylococcus aureus* and *Escherichia coli*. *Appl Environ Microbiol* 74:2171–2178
 96. Patil S, Rajiv P, Sivaraj R (2015) An investigation of antioxidant and cytotoxic properties of green synthesized silver nanoparticles. *Indo Am J Pharm Sci* 2(10):1453–1459
 97. Bhakya S, Muthukrishnan S, Sukumaran M, Muthukumar M (2015) Biogenic synthesis of silver nanoparticles and their antioxidant and antibacterial activity. *Appl Nanosci* 10:1–12
 98. Blois MS (1958) Antioxidant determinations by the use of a stable free radical. *Nature* 181:1199–1200. <https://doi.org/10.1038/1811199a0>
 99. Dipankar C, Murugan S (2012) The green synthesis, characterization and evaluation of the biological activities of silver nanoparticles synthesized from *Iresine herbstii* leaf aqueous extracts. *Colloids Surf B Biointerfaces* 98:112–119
 100. He Y, Wei F, Ma Z, Zhang H, Yang Q, Yao B, Huang Z, Li J, Zenga C, Zhang Q (2017) Green synthesis of silver nanoparticles using seed extract of *Alpinia katsumadai*, and their antioxidant, cytotoxicity, and antibacterial activities. *RSC Adv* 7:39842–39851
 101. Shanmugam C, Sivasubramanian G, Parthasarathi B, Baskaran K, Balachander R, Parameswaran VR (2016) Antimicrobial, free radical scavenging activities and catalytic oxidation of benzyl alcohol by nano-silver synthesized from the leaf extract of *Aristolochia indica* L.: a promenade towards sustainability. *Appl Nanosci* 6:711–723. <https://doi.org/10.1007/s13204-015-0477-8>
 102. Rodriguez-Gattorno G, Diaz D, Rendon L, Hernandez-Segura GO (2002) Metallic nanoparticles from spontaneous reduction of silver (I) in DMSO Interaction between nitric oxide and silver nanoparticles. *J Phys Chem B* 106(10):2482–2487
 103. Elmastas M, Gulcin I, Beydemir OI, Kufrevioglu OI, Aboul-Enein HY (2006) A study on the in vitro antioxidant activity of juniper (*Juniperus communis* L.) fruit extracts. *Anal Lett* 39:47–65
 104. Reddy N, Jayachandra D, Vali N, Rani M, Sudha Rani S (2014) Evaluation of antioxidant, antibacterial and cytotoxic effects of green synthesized silver nanoparticles by *Piper longum* fruit. *Mater Sci Eng* 34:115–122
 105. Halliwell B, Gutteridge JMC (1990) Role of free radicals and catalytic metal ions in human disease: an overview. *Methods Enzymol* 186:1–85
 106. Inbathamizh L, Mekalai Ponnu T, Jancy Mary E (2013) In vitro evaluation of antioxidant and anticancer potential of *Morinda pubescens* synthesized silver nanoparticles. *J Pharma Res* 6:32–63

Publisher's Note Springer Nature remains neutral with regard to jurisdictional claims in published maps and institutional affiliations.